第 28 卷第 8 期
2012 年 8 月

无 机 化 学 学 报
CHINESE JOURNAL OF INORGANIC CHEMISTRY

Vol.28 No.8
1755-1762

铝合金表面用化学刻蚀和阳极氧化法制备的超疏水膜层的耐蚀性能

李松梅* 李 彬 刘建华 于 美

(北京航空航天大学材料科学与工程学院,空天材料与服役教育部重点实验室,北京 100191)

摘要: 通过化学刻蚀和阳极氧化在 AA2024 铝合金表面制备超疏水表面。当化学刻蚀时间超过 3 min 时,表面在很宽 pH 值范围内显示出水静态接触角大于 150°。SEM 和 AFM 照片表明化学刻蚀时间决定了试样表面形貌和粗糙度。FTIR 用来研究氟硅烷(G502)与 AA2024 表面的结合。结果说明 FAS(氟硅烷)分子与铝合金表面的三氧化二铝发生反应,并在阳极氧化膜层表面展示出优异的结合性能。超疏水表面的耐腐蚀性能通过在质量分数为 3.5%的 NaCl 溶液中进行动电位极化和交流阻抗(EIS)测试。电化学测试结果和等效电路模型显示出超疏水表面显著改善抗腐蚀性能。

关键词: 超疏水; 化学刻蚀; 阳极氧化; 耐腐蚀

中图分类号: O647.5; O614.3+1 **文献标识码**: A **文章编号**: 1001-4861(2012)08-1755-08

Corrosion Resistance of Superhydrophobic Film on Aluminum Alloy Surface Fabricated by Chemical Etching and Anodization

LI Song-Mei* LI Bin LIU Jian-Hua YU Mei

(*Key Laboratory of Aerospace Materials and Performance, Ministry of Education, School of Materials Science and Engineering, Beihang University, Beijing* 100191, *China*)

Abstract: A superhydrophobic surface was fabricated by chemical etching and anodization on AA2024 aluminum alloy. A static water contact angle of more than 150° was achieved at a wide pH value range when the surface chemical etching time was more than 3 min. The SEM and AFM images showed that the surface morphology and roughness were dependent on chemical etching time. The FTIR results indicated that the FAS (fluorinated agent silane) molecules reacted with alundum on the aluminum alloy surface and the surface exhibited excellent adhesion performance on the anodization specimen. The corrosion resistance of the superhydrophobic surfaces was estimated by potentiodynamic polarization and electrochemical impedance spectroscopy (EIS) measurements in 3.5wt% NaCl aqueous solution. The electrochemical measurements and appropriate equivalent circuit models revealed that the anticorrosion performance was greatly improved by the superhydrophobic surface.

Key words: superhydrophobic; chemical etching; anodization; anticorrosion

Superhydrophobic surface with a water contact angle of more than 150° has drawn a great deal attention because of its potential application in the industrial area and biological process[1], such as self-clearing material[2], anti-icing coating[3], corrosion-free coating[4-5] and so on. In nature, there are many living things with superhydrophobic surfaces, such as lotus leaf, butterfly wing, etc. From the lotus leaf, we know that the superhydrophobicity of a material depends on not only its surface energy but also its surface morphology[1]. In the past decade, many methods were developed to fabricate superhydrophobic surfaces and

收稿日期:2011-11-17。收修改稿日期:2012-03-23。

航空科学基金(No.20110251003)资助项目。

*通讯联系人。E-mail:songmei_li@buaa.edu.cn

references were in the field of nano-printing[6], electrospun[7], sol-gel[8] and so on. Currently, fabrication of superhydrophobic surfaces on metal has attracted considerable research attention. For example, Wu and co-workers[9] obtained superhydrophobic surface assembly of FAS (fluorinated agent silane) molecules on rough morphology created by chemical etching. Femtosecond Laser ablation was used by Kietzig[10] et al. to create roughness on steel. Wettability of the roughness steel transformed from hydrophilicity to hydrophobicity by laying the specimen in the natural environment, and reached superhydrophobicity when the lay time was over 50 days.

Aluminum and its alloy have excellent physical and mechanical properties such as low density, good electromagnetism and high strength/weight ratio. Thus, they are expected to find applications in various industries such as aerospace and automobile. However, the poor corrosion resistance limits their application. Most of the corrosion occurs when the metallic matrix contacts with water and oxygen or other corrosion environment. One of the most effective corrosion protections for aluminum alloy is to treat the metal or alloy with chromium. However, chromium is toxic and harmful to the environment. Superhydrophobic surface treatment is one of the efficient strategies to protect aluminum alloy from corrosion because the surface is water repellent and separates the metallic matrix from water and corrosion environment. In our previous study [4], superhydrophobic surface was fabricated on aluminum alloy by anodization and self-assembly, but the method was time consuming and demanded more energy.

Here we report the preparation of superhydrophobic surface by chemical etching, anodization and self-assembly of FAS molecules. The static water contact angle was measured in wide pH value range. FTIR was employed to investigate the AA2024 surface combination of the fluorinated agent silane (FAS) molecules. Corrosion resistance of the superhydrophobic surface was estimated by electrochemical measurements in 3.5wt% NaCl aqueous solution.

1 Experimental

1.1 Preparation of superhydrophobic surface on Aluminium alloy AA2024

Aluminum alloy AA2024 (composition: 4.5% Cu, 1.5% Mg, 0.5% Fe, 0.6% Mn, 0.5% Si,0.5% others and Al is the rest) with a size of 60mm×40mm×3mm was used as the substrate. The substrates were ground by emery paper (No. 100, 500, 1000, grit sizes were 165, 25, 13 μm, respectively) gradually, and then ultrasonically cleaned in acetone and distilled water for 10 min, respectively. Diluted hydrochloric acid (V_{HCl}:V_{H_2O}=1:1) was used as chemical etching solution at 15 ℃. Chemical etching time was 2 ~4 min. Anodization process was conducted in the solution with 45 $g\cdot L^{-1}$ sulfuric acid and 10 $g\cdot L^{-1}$ boracic acid. The anodizing parameters were 0.6 $A\cdot cm^{-2}$, 25 ℃, 20 min. After anodization, the samples were immersed in 100 mL FAS solution containing 0.6 g FAS (G502, $C_{13}F_{12}H_{18}SiO_3$), 40 mL methanol and 60 mL H_2O (prepared by stirring for 4 h at 30 ℃) for 2 h at 40 ℃.

1.2 Characterization of surfaces

Water contact angles for as-prepared surfaces were estimated with optics contact angle meter (Dataphysics OCA20) based on a sessile drop measuring method. The volume of the test water droplet was 6 μL. The contact angle of samples was obtained by averaging five different points. The surface morphologies of the prepared samples were estimated by scanning electron microscope (FE-SEM, Apllo 300, Japan) and atomic force microscope (AFM, Veeco, MutiMode Nanoscope Ⅲa, USA). SEM accelerating voltage was 15 kV. The AFM test was Tapping Mode and test area was 15×15μm. Chemical bonds were characterized by Fourier transform infrared spectroscopy (FTIR; NEXUS-470, Nicolet).

1.3 Electrochemical measurements

Potentiodynamic polarization and electrochemical impedance spectroscopy (EIS) measurements were used to estimate the corrosion resistant of superhydrophobic surfaces. Electrochemical work

station (Princeton Applied Research 2273) was employed to test electrochemical measurements based on three electrode system. All electrochemical measurements were performed in 3.5wt% NaCl aqueous solutions at room temperature. Before electrochemical measurements, the specimens were immersed in the aqueous solution for 10 min to obtain a stable surface. The prepared surface was used as the working electrode with test area of 3.14 cm^2. A saturated calomel electrode was used as the reference electrode and a platinum sheet was used as the counter electrode. Potentiodynamic polarization curves were subsequently measured with respect to the open circuit potential (OCP) at a scanning rate of 2 $mV \cdot s^{-1}$ from −0.5 V to 1 V. Electrochemical impedance spectroscopic measurements were conducted in the frequency ranges between 10 mHz and 100 kHz with a sinusoidal perturbation of 10 mV. The program Zsimpwin 3.2 was used to obtain fitting parameters based on equivalent circuit.

2 Results and discussion

2.1 Fabrication of Superhydrophobic surfaces

Schemes for the sample fabrication are shown in Fig.1. All of the samples were assembled by FAS molecules. The sample only treated by chemical etching for 2, 3 and 4 min is denoted as CE2, CE3, CE4, respectively, and the sample only anodized for 20 min is denoted as A, and the samples treated by chemical etching for 2, 3 and 4 min and anodization for 20 min is named as CE2A, CE3A and CE4A, respectively. Fig.2 shows the water contact angle measurement on samples obtained by different treatments under wide pH value range. It can be seen clearly that the surfaces anodized for 20 min (A) has the lowest water contact angle from 90° to 100° in all pH value ranges. The surface chemical etching for 2 min (CE2) has water contact angle values from 132° to 139°, and exhibits hydrophobic property, so is the surface treated by chemical etching for 2 min and by anodization for 20 min (CE2A). The contact angle is greater than 150° if chemical etching time for the sample is over 3 min (CE3, CE4, CE3A and CE4A). The water contact angle has a little decrease when the pH value of water is above 9.

Thus we can conclude that in the process of superhydrophobic surfaces preparation, the determining factor is chemical etching. The wettability of the surfaces changes with chemical etching time. The wettability of the surfaces becomes more hydrophobic by extending chemical etching time. Water contact angle does not show any further variations when chemical time is over 3 min. As shown in Fig.1, the morphology of the surfaces is altered by chemical etching. These can be observed by FE-SEM photographs and AFM images in the next section. The surface chemical property is changed by anodization and self-assembly. This will be discussed

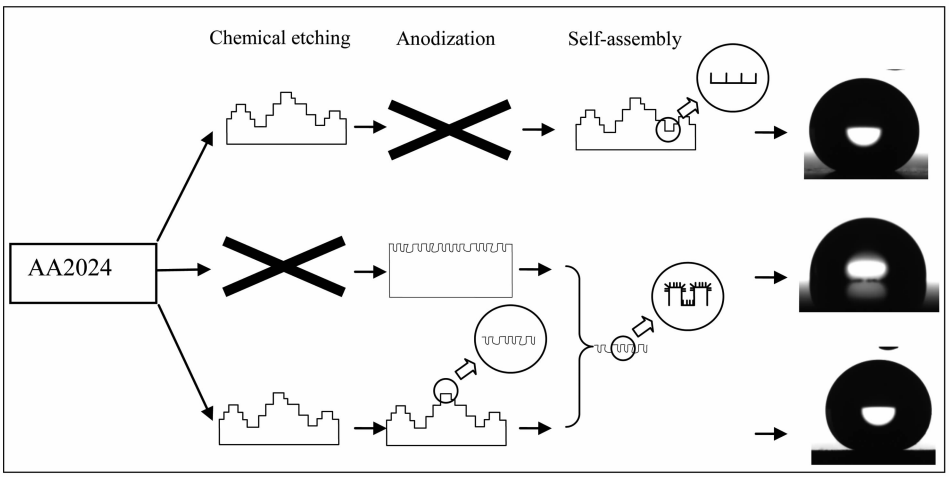

Fig.1　Schematic diagram of different processes to obtain different surfaces and related typical optics contact angle

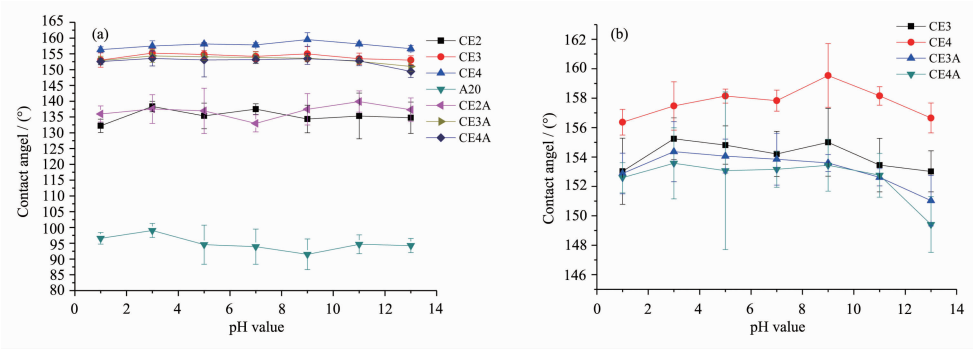

Fig.2 Water contact values measured on several samples treated by different technologies

in the chemical characterization section.

2.2 Morphology of the surfaces

FE-SEM photographs and 3-D top AFM images of several samples are shown in Fig.3. (a), (b) and (c) are the FE-SEM photographs for sample CE2, CE3 and CE4, respectively. It can be seen from Fig.3 (a) that the surface of the sample by chemical etching for 2 min is not destroyed totally. There exist platforms from the pretreatment in preparation and a few grooves from etching by dilute chlorhydric acid on the surfaces. As a contrast, Fig.3 (b) and (c) are the images of CE3 and CE4. The surfaces are completely destroyed by dilute chlorhydric acid and become rough. There are irregularly shaped particles on the

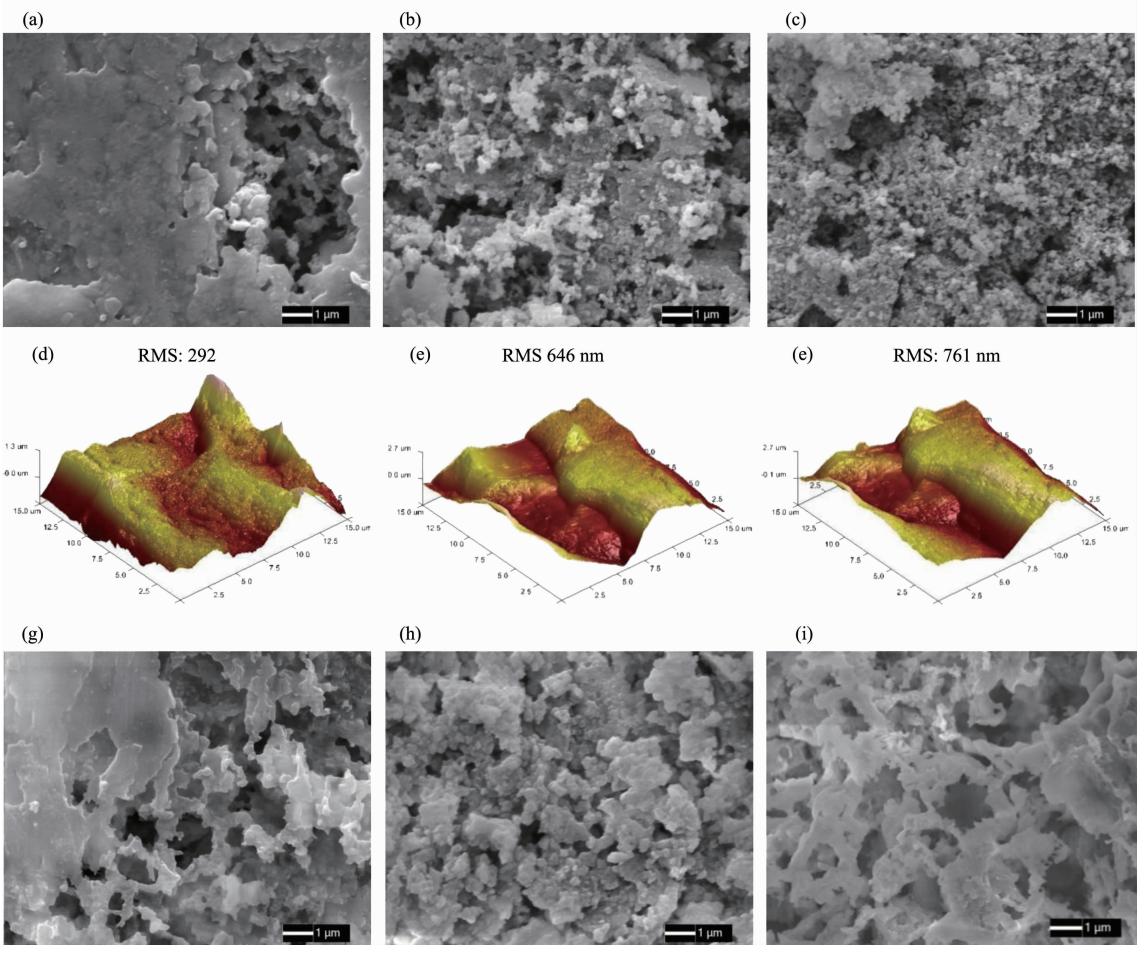

Fig.3 FE-SEM image of (a) CE2, (b) CE3, (c) CE4, (g) CE2A, (h) CE3A, (i) self-assembled of CE3A and 3-D top AFM images of (d) CE2, (e) CE3, (f) CE4

surfaces. Fig.3 (d), (e) and (f) are the 3-D top AFM images of the sample CE2, CE3 and CE4, respectively. From the AFM images we know the RMS (Roughness Measurement of the Surface) of CE2, CE3 and CE4 is 292 nm, 646 nm and 761 nm, respectively. When chemical etching time is just 2 min, the RMS is only 292 nm. The RMS value of CE3 is 646 nm, which is double of the sample CE2. The RMS value has continued to increase with chemical etching time. There is no difference between CE2 (Fig.3 (a)) and CE2A (Fig.3 (g)), and there is also no distinction between CE3 (Fig.3 (b)) and CE3A (Fig.3 (h)). It demonstrates that the self-assembly does not change the morphology of aluminum alloy surfaces when compared the Fig.3(h) and (i).

In summary, chemical etching plays an essential role in changing morphologies and RMS. In contrast to chemical etching, anodization does not have any effects on the morphology. When chemical etching time is 3 min, the surface of aluminum alloy is destroyed by dilute chlorhydric acid, and the water contact angle of the surfaces reaches 150° no matter the specimen is treated by anodization or not.

2.3 Chemical characterization of superhydrophobic

Fig.4 shows the FTIR spectra of several samples. From the whole spectrum of the sample anodized without self-assembly of FAS molecules (Fig.4(a)), one can see that there is only one peak at 1 138 cm^{-1} due to Al-O-Al stretching modes. Fig.4 (b) is the spectrum of the sample self-assembled by FAS molecules on anodization AA2024, there are two peaks at 1 127 cm^{-1} and 1 160 cm^{-1}, assigned to Si-O and Al-O-Si, respectively. There is one more peak at 1 245 cm^{-1} assigned to $-CF_2$ and $-CF_3$. These peaks demonstrate that FAS molecules are assembled on anodized AA2024. There are no any peaks in the spectrum for the sample self-assembled by FAS molecules on chemical etched AA2024 (CE3) as shown in Fig.4(c). It demonstrates that there are little FAS molecules on chemical etched AA2024 (CE3). There are three peaks for the sample self-assembled by FAS molecules on chemical etched and anodized AA2024 (CE3A) at 1 116 cm^{-1}, 1 141 cm^{-1} and 1 241 cm^{-1}, respectively, almost the same as that of the self-assembled FAS molecules on anodized AA2024, which is obvious in Fig.4(b) and (d). The peak at 1 241 cm^{-1} is assigned to $-CF_2$ and $-CF_3$, and the peaks at 1 116 cm^{-1} and 1 141 cm^{-1} are assigned to Si-O and Al-O-Si, respectively, the same as that of the self-assembled FAS molecules on anodized AA2024. These peaks demonstrate that FAS molecules are assembled on the sample treated with chemical etching and anodization.

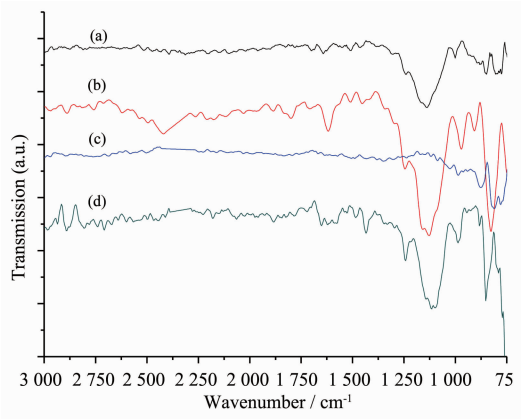

Fig.4 FTIR spectra of (a) anodized AA2024, (b) self-assembly of FAS molecules on anodized AA2024, (c) self-assembly of FAS molecules on chemical etched AA2024 (CE3), (d) self-assembly of FAS molecules on chemical etched and anodized AA2024 (CE3A)

It can be seen from the FTIR spectra that the FAS molecules are assembled on the specimen treated by anodizing. Anodization film on aluminum alloy is a must for self-assembly. Fadeev et al[11] have demonstrated that the FAS molecules reacted with the hydroxyl group on the solid surface have several modes. Hydroxyl group is the pre-requirement for FAS molecules to react with solid surfaces. Takahiro Ishizaki and his co-workers [5,12] have assembled fluoroalkylsilane molecules on magnesium alloy coated with nano-structured cerium oxide lm. The hydroxyl group on the cerium oxide is bonded with fluoroalkylsilane. Liu et al[13] used n-tetradecanoic acid (CH_3 $(CH_2)_{12}COOH$) to assemble on the copper sheet treated with 7 mol·L^{-1} HNO_3 for 30 seconds to activate surfaces. The above examples demonstrate that the hydroxyl group is the most important factor in

self-assembly. In our study, the hydroxyl group for assembly is provided by anodization, and there are little FAS molecules assembled on the samples treated by chemical etching only.

2.4 Corrosion resistant performance of the superhydrophobic surface

The corrosion resistant performance of the superhydrophobic surfaces was investigated in NaCl aqueous solution from the electrochemical point of view. Fig.5 shows potentiodynamic polarization curves of (a) bare Al, (b) anodization, (c) CE2A and (d) CE3A immersed in 3.5wt% NaCl aqueous solution. As compared to the corrosion current density (j_{corr}) of the bare aluminum alloy (1.386×10^{-7} A·cm^{-2}), that of the specimen treated by anodization (1.15×10^{-10} A·cm^{-2}) decreases by more than three orders of magnitude. The j_{corr} values of the surfaces CE2A and CE3A are estimated to be 2.89×10^{-10} A·cm^{-2} and 8.509×10^{-12} A·cm^{-2}, respectively. It should be noted that the j_{corr} value of CE3A decreases by five orders of magnitude compared with that of bare aluminum alloy. This supports the conclusion that the superhydrophobic treatment is effective for improving the corrosion resistance of aluminum alloy. In addition, the corrosion potential (E_{corr}) of the bare aluminum, anodization samples, CE2A and CE3A are −637 mV, −498 mV, −420 mV and −577 mV, respectively. As compared to the E_{corr} values of the bare aluminum specimen, that of the superhydrophobic surfaces (CE3A) are shifted to the positive direction. The significant shift of the E_{corr} to the positive direction could be attributed to an improvement in the

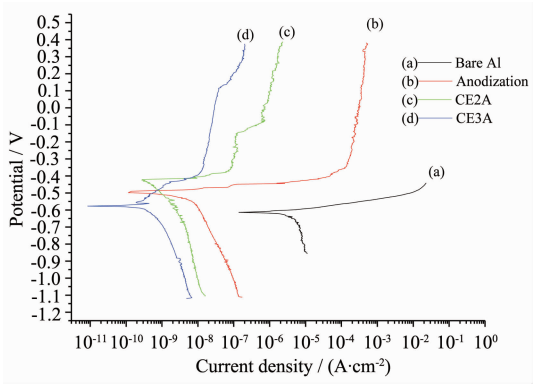

Fig.5 Polarization curves of (a) bare Al, (b) anodization, (c) CE2A and (d) CE3A immersion in 3.5wt% NaCl aqueous solution

protective properties of the superhydrophobic surfaces on aluminum alloy. We can draw the same conclusion from the j_{corr} and E_{corr} numerical data that the corrosion resistant performance of aluminum alloy is greatly improved by superhydrophobic surface treatment.

Fig.6 presents the EIS bode plots of the samples of (a) bare Al, (b) anodization, (c) CE2A and (d) CE3A immersed in 3.5wt% NaCl aqueous solution. Generally, we consider the |Z| values at low frequency as some point of anticorrosion performance. The |Z| values at 10 mHz of (a) bare Al, (b) anodization, (c) CE2A and (d) CE3A immersed in 3.5wt% NaCl aqueous solution are 4.94 kΩ·cm^2, 3.20 MΩ·cm^2, 15.4 MΩ·cm^2 and 33.2 MΩ·cm^2, respectively. The |Z| value of superhydrophobic surfaces (CE3A) at 10 mHz decreases by 4 orders of magnitude when compared with that of the bare aluminum. It should be noted that the |Z| value of superhydrophobic surfaces (CE3A) in 10 mHz is just two times that of CE2A,

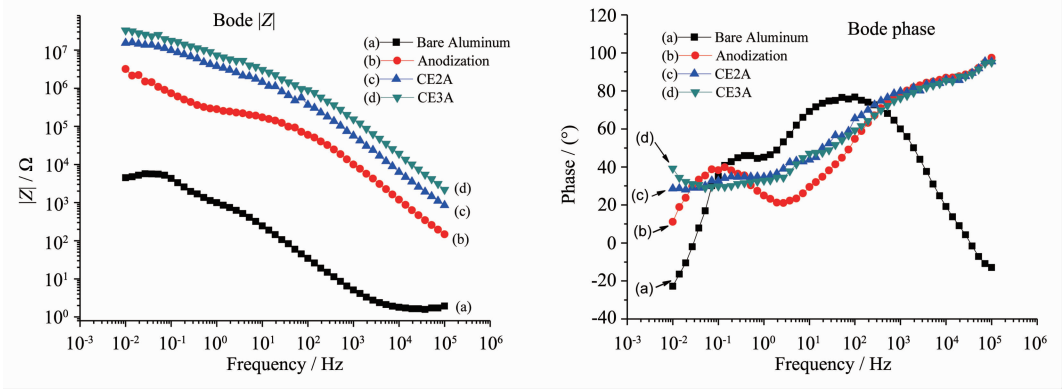

Fig.6 Bode plots for (a) bare Al, (b) anodization, (c) CE2A and (d) CE3A immersion in 3.5wt% NaCl aqueous solution

however, it is decuple that of anodization. These results indicate that superhydrophobic treatment tremendously improves anticorrosion performance. As compared to the |*Z*| value of the specimen treated with anodization, that of the specimen treated with both chemical etching and anodizing (CE2A, CE3A) raises one order of magnitude. It indicates that changing wettability of aluminum alloy surfaces could improve their anticorrosion performance.

It can be seen from Fig.6 that the impedance spectra of bare aluminum and the specimen treated with anodizing have two capacitive loops at medium and low frequency. For the specimen treated with anodizing, the medium loop shifts to higher frequency, and the low loop shifts to lower one. This is because that the structure of aluminum surfaces has been changed by anodization and self-assembly of FAS molecules. The medium loop can be attributed to the natural oxide (anodization and self-assembly of FAS molecules) films on the electrode surface, while the other loop can be attributed to the double layer capacitance. The impedance spectra of CE2A and CE3A have a similar plot with three capacitive loops at high, medium and low frequency, respectively. The loop at high frequency can be attributed to air layer between solid surfaces and solution created by roughness structure on superhydrophobic surfaces, the medium one can be attributed to anodization and self-assembly, and the last one can be due to double layer. This conclusion is well in agreement with the FE-SEM image results.

To further determine accurate analysis of the impedance data, the equivalence circuit models are proposed. As shown in Fig.7, the equivalent circuit model (a) is for bare aluminum and anodization (A), and (b) is for CE2A and CE3A immersed in 3.5wt% NaCl aqueous solution. In these circuit models, $R_{ct}||C_{dl}$ is assigned to the impedance of the interface reaction between the films and substrate, $R_c||C_c$ is assigned to the impedance of the interface

$C_{air}||R_{air}$ is assigned to the air layer from reaction between the electrolytic solution and films, and trapped by rough structures of the superhydrophobic surfaces. There are no pores on bare aluminum and anodization (A) specimen, so the equivalent circuit model (a) can be used to fitting them. Equivalent circuit model (b) can be used for fitting hydrophobic surfaces. The R_{ct} values obtained from the fitting results as a corrosion resistant emblem are shown in Table 1. The R_{ct} values of bare aluminum, anodization (A), CE2A and CE3A are 4.44 kΩ·cm^2, 1.85 MΩ·cm^2, 12.3 MΩ·cm^2 and 34.2 MΩ·cm^2, respectively, almost with the same order of magnitude as |*Z*| values of electrochemical impedance spectroscopy at 10 mHz. It indicates that our equivalent circuit models are well suited for the electrochemical impedance spectroscopy. Compared the specimen treated with anodization to the bare aluminum, R_c has increased by 3 orders of magnitude, and R_{ct} value has also increased by 3 orders of magnitude. These results indicate that anodization and self-assembly of FAS molecules improve anticorrosion resistance of aluminum, the same conclusion as the |*Z*| values for electrochemical impedance spectroscopy at 10 mHz and the potentiodynamic polarization curves. Compared the R_{ct} values of CE2A and CE3A with the

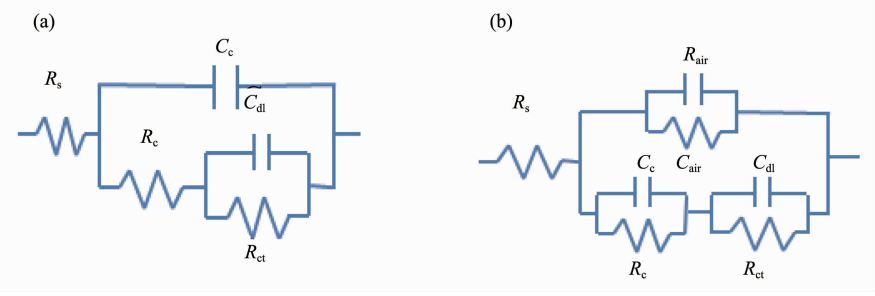

Fig.7　Equivalent circuit models of the studied system for (a) bare Al and anodization, (b) CE2A and CE3A immersed in 3.5wt% NaCl aqueous solutions

Table 1 Electrochemical model impedance parameters from Nyquist plots of different samples

	R_s / ($\Omega\cdot cm^2$)	C_{air} / ($F\cdot cm^{-2}$)	R_{air} / ($\Omega\cdot cm^2$)	C_c / ($F\cdot cm^{-2}$)	R_c / ($\Omega\cdot cm^2$)	C_{dl} / ($F\cdot cm^2$)	R_{ct} / ($\Omega\cdot cm^2$)	R_{10mHz} / ($\Omega\cdot cm^2$)
Bare Al	1.95	–	–	4.30×10^{-5}	8.07×10^{2}	2.21×10^{-4}	4.44×10^{3}	4.94×10^{3}
Anodization	21.6	–	–	1.50×10^{-8}	2.21×10^{5}	1.98×10^{-6}	1.85×10^{6}	3.20×10^{6}
CE2A	16.7	8.17×10^{-9}	1.21×10^{6}	2.70×10^{-9}	4.00×10^{6}	1.49×10^{-7}	1.23×10^{7}	1.54×10^{7}
CE3A	24.5	1.15×10^{-8}	3.81×10^{6}	1.12×10^{-9}	1.08×10^{7}	3.26×10^{7}	3.42×10^{7}	3.32×10^{7}

R_{ct} of anodization (A), it can see that the anticorrosion performance is improved by wettability of the aluminum alloy surfaces, which is the same as $|Z|$ values for electrochemical impedance spectroscopy at 10 mHz. When compared the R_{air} values of CE3A with that of CE2A, it is also found that the anticorrosion performance is influenced by wettability of aluminum surfaces.

3 Conclusions

This paper has demonstrated a convenient and effective method to prepare superhydrophobic surfaces by means of chemical etching and anodization. A static water contact angle of more than 154 at a wide pH value range can be obtained when the as-prepared surfaces are self-assembled by FAS molecules. Chemical etching time is the critical factor for the surface morphology and the water contact angle. Anodization is a necessary process for fabrication of superhydrophobic surfaces. Moreover, the superhydrophobic surfaces exhibit excellent anticorrosion performance compared with the anodization samples and the bare samples when just applying immersion in the corrosion environment for 30 min.

References:

[1] Ma M, Hill R M. *Curr. Opin. Colloid In.*, **2006**,**11**(4):193-202

[2] Li X, Du X, He J. *Langmuir*, **2010**,**26**(16):13528-13534

[3] Mishchenko L, Hatton B, Bahadur V, et al. *ACS Nano*, **2010**,**4**(12):7699-7707

[4] LI Song-Mei(李松梅), ZHOU Si-Zhuo(周思卓), LIU Jian-Hua(刘建华). *Acta Phys.-Chim. Sin.*(*Wuli Huaxue Xuebao*), **2009**,**25**(12):2581-2589

[5] Ishizaki T, Masuda Y, Sakamoto M. *Langmuir*, **2011**,**27**(8):4780-4788

[6] Weng C, Chang C, Peng C, et al. *Chem. Mater.*, **2011**,**23**(8):2075-2083

[7] Grignard B, Vaillant A, de Coninck J, et al. *Langmuir*, **2011**,**27**(1):335-342

[8] Lu S, Chen Y, Xu W, et al. *Appl. Surf. Sci.*, **2010**,**256**(20):6072-6075

[9] Xu W, Liu H, Lu S, et al. *Langmuir*, **2008**,**24**(19):10895-10900

[10]Kietzig A, Hatzikiriakos S G, Englezos P. *Langmuir*, **2009**, **25**(8):4821-4827

[11]Fadeev A Y, Mccarthy T J. *Langmuir*, **2000**,**16**(18):7268-7274

[12]Ishizaki T, Hieda J, Saito N, et al. *Electrochim. Acta*, **2010**, **55**(23):7094-7101

[13]Liu T, Chen S, Cheng S, et al. *Electrochim. Acta*, **2007**,**52**(28):8003-8007